Journal of Bioenergetics and Biomembranes, Vol. 18, No. 6, 1986

Cation-Induced Aggregation of Membrane Vesicles Isolated from Vascular Smooth Muscle

Chiu-Yin Kwan[1]

Received February 28, 1986; revised May 5, 1986

Abstract

Cations stimulated aortic muscle membrane aggregation with increasing potency according to their effective charge, e.g., $K^+ < Mg^{2+} < La^{3+}$, and the stimulation is reciprocally related to the apparent affinity for these cations. Divalent metal ion-induced membrane aggregation showed a dependence on the ionic radius, being optimal for Cd^{2+}. Polyvalent cation-induced membrane aggregation was reversibly suppressed by high ionic strength as well as by metal ion chelators, irreversibly inhibited by the cross-linking agent glutaraldehyde, and enhanced by increasing concentrations of ethanol and increased temperature of the medium. When the pH is lowered below 6.0, membrane aggregation progressively increased with a concomitant decrease in cation-induced aggregation. The patterns of aggregation of microsomal membranes and further purified plasma membranes were almost identical whereas the aggregation of the heterogeneous mitochondrial membrane-enriched fraction was distinctly different in the initial rate of aggregation, its pH dependence, and metal ion concentration dependence. Our results indicate that cation-induced membrane aggregation can also be used to isolate a plasma membrane-enriched fraction from vascular smooth muscle.

Key Words: Membrane aggregation; smooth muscle plasma membranes; calcium; blood vessels.

Introduction

It is well recognized that divalent metal ions, such as Ca^{2+} in particular, can promote aggregation and fusion of biological membranes (Papahadjapolous *et al.*, 1979; Wilshut *et al.*, 1981). Since membrane aggregation is brought about by the close contact of at least two membrane surfaces, the aggregation phenomena may represent the primary process leading to the more com-

[1]Smooth Muscle Research Program, Department of Neurosciences, McMaster University Health Sciences Center, 1200 Main Street West, Hamilton, Ontario L8N 3Z5, Canada.

0145-479X/86/1200-0487$05.00/0

plicated mechanisms of cell-to-cell interactions. Artificial membranes have generally been employed as simplified membrane model systems to investigate the mechanism of the aggregation process at the molecular level using various biophysical techniques (Wilshut *et al.*, 1981). Information on the aggregation of biological membranes, on the other hand, is rather limited. Haynes and his colleagues have reported that Ca^{2+} caused aggregation of isolated chromaffin granule membranes (Morris *et al.*, 1979) and Torpedo electric organ synaptic vesicles (Haynes *et al.*, 1979) with an apparent dissociation constant of 4–5 mM for Ca^{2+}. A similar finding was also observed by Ohyashiki *et al.* (1984) using brush border membrane vesicles isolated from pig intestine. Although microsomal membrane and plasma membrane vesicles have been isolated from several types of smooth muscle and employed to study membrane-related biochemical events such as ligand–receptor interactions, ion transport, and related ATPases (Grover *et al.*, 1984; Kitabgi *et al.*, 1984; Daniel *et al.*, 1982; Kwan and Kostka, 1983, 1984; Kwan *et al.*, 1984a), their use to study membrane aggregation has not been reported in spite of the fact that smooth muscle cells do elicit secretory process (Gabella, 1981), which involves initial membrane contact with subsequent membrane fusion. In this communication, evidence is presented to indicate that a broad spectrum of cations can induce aggregation of plasmalemmal microsomes isolated from canine aortic smooth muscle, and the factors affecting the membrane aggregation processes are examined. The results further suggest that usefulness of using aggregation phenomenon to prepare vascular muscle plasma membranes.

Materials and Methods

Preparation of Microsomal and Other Subcellular Membranes

Microsomal membrane fractions (MIC) enriched in plasma membrane vesicles were prepared from the canine aortic smooth muscle by differential centrifugation according to the method previously described in detail (Kwan *et al.*, 1984b). In some experiments the mitochondrial membrane-enriched fraction (P1) and the highly purified plasma membrane fraction (F2) obtained as a microsomal subfraction from the discontinuous sucrose density gradient at the interphase of 15 and 30% sucrose layers were also employed. The folds of enrichment of P1, MIC, and F2 over the initial total membrane fraction, postnuclear supernatant (PNS), were 2, 6, and 20 respectively in 5′-nucleotidase and phosphodiesterase I activities (plasma membrane markers), and 7, 2, and 1 in cytochrome *c* oxidase activities (mitochondrial membrane markers). NADPH-cytochrome *c* reductase activities in these

three fractions were comparable and were 4- to 5-fold enriched over that in PNS. Detailed characterization of these subcellular membrane fractions from dog aortic smooth muscle has been reported elsewhere (Kwan *et al.*, 1984b). Since the smooth muscle was homogenized in isotonic medium containing 8% sucrose and 10 mM imidazole buffer, pH 7.5, the isolated plasmalemmal microsomes were also resuspended and stored in the same medium.

Measurement of Membrane Aggregation

Membrane aggregation was monitored turbidimetrically at 450 nm by continuous measurement of the optical density changes of the membrane suspensions (Ohyashiki *et al.*, 1984; Ohyashiki and Mohri, 1983) with a Beckman spectrophotometer equipped with temperature control. To 0.95 ml of the membrane suspension containing 100–200 μg protein in the isotonic sucrose-imidazole medium (pH 7.5, 25°C) aliquots of concentrated salt solutions (100 mM–1 M) were added to initiate the aggregation process. A small variation due to the dilution by added solution was less than 5% and was not corrected. Other measuring conditions are specified in the corresponding figure legends. Rapid mixing can be effectively achieved in a few seconds by up-and-down suction actions using a pipette without removal of the cuvette from the cell holder. Caution was taken not to introduce air bubbles during mixing. Unless otherwise stated, most endpoint readings of optical density were done at 3 min after the induction of membrane aggregation and were corrected for the basal optical density of the membranes before the induction of membrane aggregation.

The increased turbidity of membrane fractions was not due to osmotic shrinkage of membrane vesicles because addition of high concentrations of sucrose (up to 30%) failed to increase the turbidity. Increased turbidity was accompanied by an increased amount of membrane sediments (centrifuged at 10,000 $\times$ *g* for 10 min) as reflected by the increased protein content. It was not due to fusion of vesicles because under most experimental conditions the turbidity changes were reversible (see Results).

Chemical Reagents

All reagents were of analytical grade. Chloride salts of all inorganic cations used were purchased from either Sigma or Fischer. All solutions were prepared using deionized and distilled water. Buffer solutions were pretreated with chelax-100 resin to remove contaminating metal ions. Metal ion chelators, ethylenediamine tetraacetic acid (EDTA) and ethylene glycol-bis-(aminoethylether)-*N*,*N*′-tetraacetic acid (EDTA), were prepared in water and titrated to about pH 7–8 before use.

Results

The Time Course of Cation-Induced Membrane Aggregation

Figure 1 shows that the addition of K^+, Mg^{2+}, and La^{3+} to the membrane suspension caused an initial rapid formation of membrane aggregates which reached 80% of the plateau level in approximately 1 min. The subsequent slow increase in the turbidity leveled off at approximately 5 min and remained unchanged for at least 60 min. Longer than 60 min of incubation resulted in a slow decrease in turbidity which was due to the precipitation of a higher order of membrane aggregates as was visibly detectable. This result also shows that the highest level of membrane aggregation occurred with relatively much lower concentration of trivalent cations whereas the monovalent cation at much higher concentration had only a slight effect in promoting the membrane aggregation. Figure 2 shows that such cation-induced increase in the turbidity of membrane suspension was linearly related to the increasing concentration of membrane protein over a wide range, indicating a membrane aggregation process.

The Effects of Various Divalent Metal Ions

To study the specificity of the membrane aggregation induced by divalent metal ions, several divalent cations in addition to Mg^{2+} were tested. Figure 3 shows that 10 mM concentration of seven different divalent metal ions caused various degrees of membrane aggregation with similar time course. The inset shows the dependence of the membrane aggregation on the

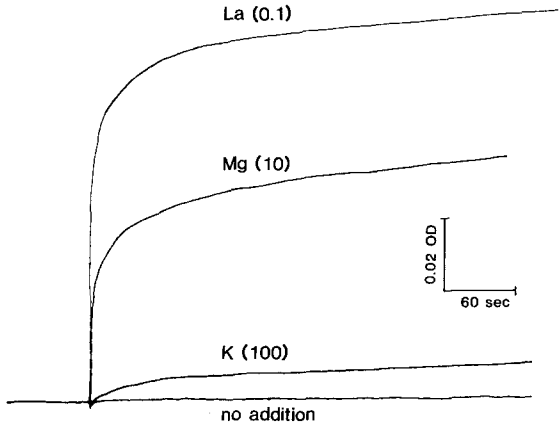

Fig. 1. The time course of optical density changes at 450 nm of microsomal membrane suspension (89 μg/ml) upon addition of cations. Numbers in the parentheses indicate the final concentration (mM) of cations.

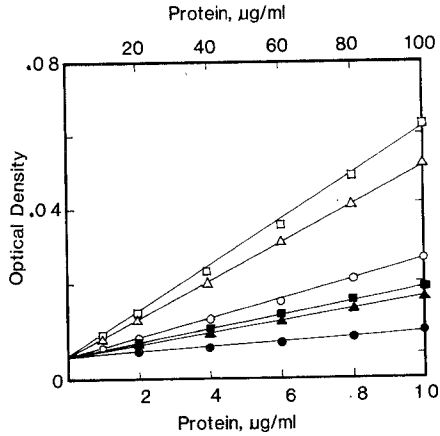

Fig. 2. Protein concentration dependence of optical density changes of microsomal membrane suspension in the presence of 10 mM Mg^{2+} (open symbols, top scale) and 0.1 mM La^{3+} (closed symbols, bottom scale). Optical densities were measured at 450 nm just before the addition of cations (circles), 30 sec (triangles), and 5 min (squares) after the addition of cations.

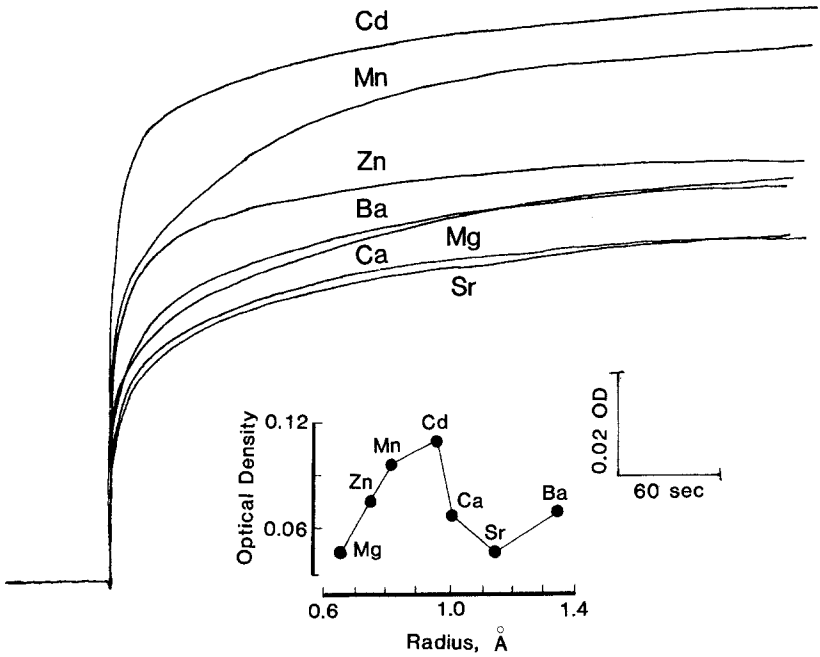

Fig. 3. The optical changes of microsomal membrane suspension in the presence of various divalent metal ions (all in 10 mM final concentration). Inset: Optical density was measured 3 min after the induction of membrane aggregation by adding concentrated divalent metal ions to microsomal membrane suspension containing 92 μg/ml protein.

ionic radius of these divalent cations, with Cd^{2+} (0.98 Å) being the optimal size.

The Dependence of the Cation Concentration

Figure 4 shows the titration profiles of membrane aggregation as a function of the concentration of cations employed. There was a striking difference among these cations in their concentrations required to cause half-maximal membrane aggregation ($K_{0.5}$). The $K_{0.5}$ for La^{3+}, Cd^{2+}, Mg^{2+}, and K^+ were 25 μM, 0.2 mM, 2.0 mM, and 20 mM, respectively. The titration profile for La^{3+} was different from those of other cations in that it followed a sigmoidal pattern as opposed to a hyperbolic pattern.

The Effect of Ionic Strength of the Medium

The results so far suggest that ionic interactions between the cations and the negative changes of the membrane surfaces seem to be the driving force that brings about the aggregation of membrane vesicles. If so, increasing the ionic strength of the medium would weaken such ionic interactions. Figure 5 shows this was exactly the case with smooth muscle membrane vesicles. Addition of 100 mM K^+ to the membrane suspension substantially reversed

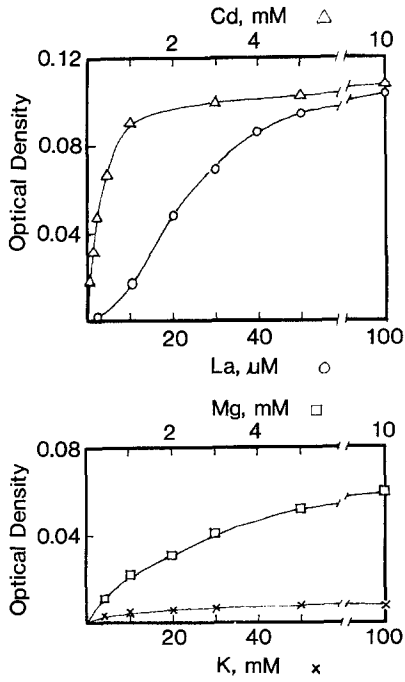

Fig. 4. Cation concentration dependence of the aggregation of the microsomal membrane suspension (87 μg/ml). Conditions were the same as described in the legend of Fig. 3.

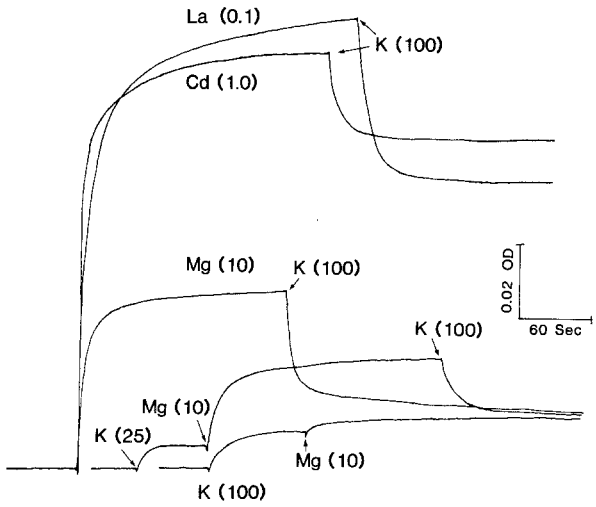

Fig. 5. The effect of high K^+ concentration on the divalent cation-induced aggregation of microsomal membranes. Numbers in the parentheses indicate the final concentration (mM) of cations.

the membrane aggregation already formed in the presence of 10 mM Mg^{2+} and prevented the Mg^{2+}-induced membrane aggregation if K^+ was added before Mg^{2+}. This effect, due to ionic strength, was reversible. Although a partial effect was observed for La^{3+}- or Cd^{2+}-induced membrane aggregation, an almost complete reversal or prevention of membrane aggregation by high K^+ concentration was observed in Mg^{2+}-induced membrane aggregation. The residual turbidity was mainly due to the low level of membrane aggregation caused by 100 mM K^+ itself (see Fig. 6). The action of high K^+

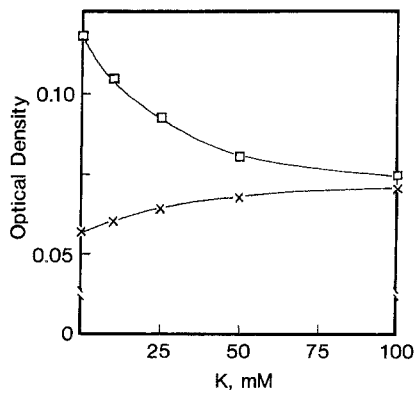

Fig. 6. K^+ concentration dependence of aggregation of microsomal membranes (92 μg/ml) in the presence of (□) and absence (x) of 10 mM Mg^{2+}. The basal optical density changes in the absence of 10 mM Mg^{2+} were not corrected for the total optical density readings represented by square symbols.

concentration may be partially due to competition for the divalent cation binding sites in the membrane. However, increasing the ionic strength of the medium by raising the imidazole concentration from 10 to 100 mM produced the same effect as high K^+ (see also below).

The Effect of Ethanol on Mg^{2+}-Induced Membrane Aggregation

In contrast to the effect of high ionic strength of the aqueous medium which weakens the ionic interactions between two oppositely charged centers, lowering of the polarity of the aqueous medium would strengthen such ionic interactions. This basic physical principle should be applicable to our system, if the cation-induced membrane aggregation is indeed promoted by the ionic interactions. Figure 7 clearly shows that this was true. As the polarity of the

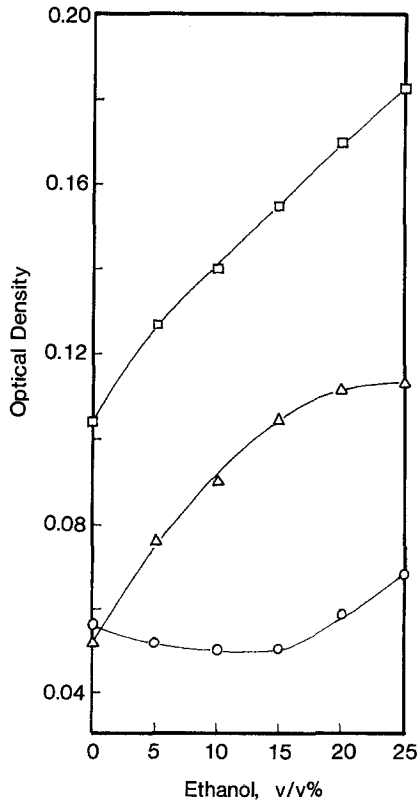

Fig. 7. The effect of ethanol on the aggregation of microsomal membranes (92 μg/ml) in the presence (□) and absence of (○) of 10 mM Mg^{2+}. Triangular symbols represent the difference between □ and ○. Ethanol solutions were mixed with equal volume of sucrose-imidazole (twice concentrated in sucrose and imidazole concentrations) buffer solution to achieve the desired ethanol concentration (V%).

aqueous medium of the membrane suspension was progressively lowered by the addition of increasing concentrations of ethanol, a remarkable increase of the level of Mg^{2+}-induced membrane aggregation was observed, 20–25% (v/v) ethanol being optimal for such an effect. In the absence of added Mg^{2+}, a much higher threshold ethanol concentration was required to initiate membrane aggregation. However, ethanol may also act via perturbation of membranes by increasing membrane fluidity. Therefore, the effect of elevation of temperature which causes increased membrane fluidity was also studied.

The Effect of Temperature on Mg^{2+}-Induced Membrane Aggregation

Figure 8 shows that increasing the temperature from 23 to 42°C caused a marked increase in Mg^{2+}-induced membrane aggregation which is most prominent in the temperature range 32–42°C. Although Mg^{2+}-induced membrane aggregation was enhanced under both conditions of increasing ethanol concentration and increasing temperature, the $K_{0.5}$ values for Mg^{2+} were quite different. Figure 9 indicates that $K_{0.5}$ decreased from approximately

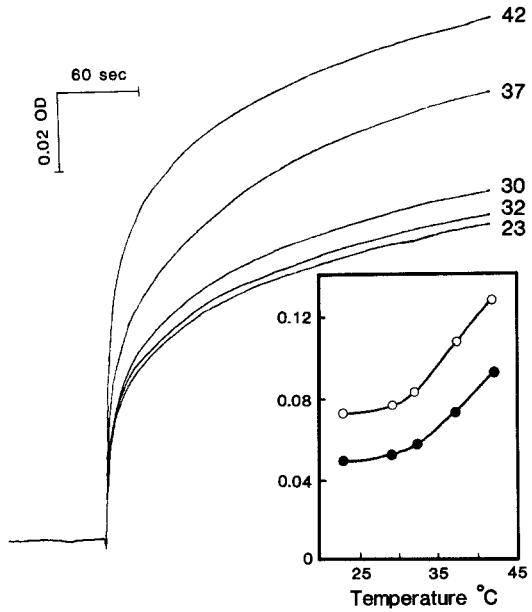

Fig. 8. The effect of temperature on the aggregation of microsomal membranes (89 μg/ml). Optical densities at 450 mm were measured 30 sec (●) and 3 min (○) after the addition of 10 mM Mg^{2+}. It is assumed that addition of 10 μl (1% of the final volume) of concentrated Mg^{2+} solution at ambient room temperature did not significantly affect the equilibrium temperature of the buffer solution containing the membranes.

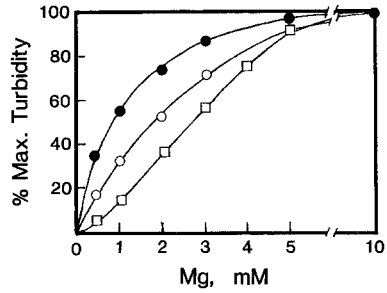

Fig. 9. Mg^{2+} concentration dependence of microsomal membrane aggregation at 23°C (○), 37°C (□), and 23°C in the presence of 20% (v/v) ethanol (●). Conditions were similar to those described in the legend of Figs. 7 and 8.

2 to 0.8 mM in the presence of 20% ethanol, whereas it increased to 3 mM at 37°C. The changes of $K_{0.5}$ under these conditions were not remarkable but the results are consistent with the notion that ionic interactions between Mg^{2+} and the membrane vesicles were enhanced in the medium of lower polarity and weakened at higher temperature.

The Effect of Cross-Linking of Membrane Proteins

To investigate the role of membrane proteins in the aggregation phenomenon, the membrane proteins were cross-linked with glutaraldehyde (GA). Figure 10 shows that addition of GA to the membrane suspension before the addition of Mg^{2+} failed to show Mg^{2+}-induced membrane aggregation. Such a prevention by GA of cation-induced membrane aggregation was not reversible because membrane aggregation induced by 10 mM Mg^{2+}

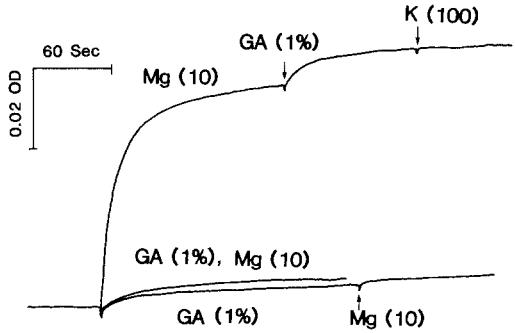

Fig. 10. The effect of glutaraldehyde (GA) on the aggregation of microsomal membranes (76 μg/ml). Note that 1% GA prevented the suppression of Mg^{2+}-induced aggregation by high concentration of K^+ and, if added before Mg^{2+}, GA also prevented the Mg^{2+}-induced aggregation. Glutaraldehyde was added as concentrated stock solution at 23°C.

was not reversed by subsequent addition of GA. On the contrary, GA further increased the level of membrane aggregation if added after the induction of membrane aggregation by Mg^{2+}. Addition of 100 mM KCl or EDTA, which normally reversed the Mg^{2+}-induced membrane aggregation in the absence of GA, did not reverse the Mg^{2+}-induced membrane aggregation after cross-linking by GA. Furthermore, 10 mM Mg^{2+} failed to induce aggregation of GA-treated membrane vesicles.

The Effect of Chelating Agents and pH

To test the reversibility of divalent metal cation-induced membrane aggregation, 10 mM EGTA was added to the membrane aggregates which were formed in the presence of 10 mM Ca^{2+}. Figure 11 shows that addition of EGTA did not reverse but rather enhance the Ca^{2+}-induced membrane aggregation (trace a). Measurement of the pH before and after addition of EGTA revealed a remarkable drop of pH from 7.5 to 5.0 as a result of proton release upon complexation between Ca^{2+} and EGTA. Titration of the membrane suspension from pH 5.0 to 7.1 with NaOH substantially reversed the membrane aggregation. One way to prevent such a large drop of pH upon addition of EGTA is by increasing the buffer capacity from 10 mM imidazole to 100 mM imidazole (trace b). It is evident that under this condition, addition of EGTA caused an almost complete reversal of Ca^{2+}-induced membrane aggregation, and the pH of the membrane suspension dropped slightly by only 0.25 pH unit. The lower level of membrane aggregation induced by 10 mM Mg^{2+} in 100 mM imidazole compared to that in 10 mM imidazole is likely due to the increase of ionic strength (see Fig. 6). An alternative way to circumvent the change of pH in 10 mM imidazole buffer is to pretitrate the solution containing Ca^{2+} and EGTA with NaOH to about pH 7.5 before adding to the membrane suspension. The Ca^{2+}-induced membrane aggregation was completely prevented by the presence of EGTA, and the pH of the membrane suspension remained unaltered (tracing c). Decreasing the pH of the membrane suspension by HCl titration stimulated the membrane aggregation. For comparison, tracing d shows that the addition of untitrated Ca–EGTA solution to the membrane solution caused remarkable membrane aggregation (similar to tracing a) which was reversible by changes of pH.

The Effect of pH on Aggregation of Different Subcellular Membranes

The previous data suggest that proton may also modulate the membrane aggregation. Since mitochondrial and microsomal membranes of smooth muscle are different in protein and perhaps lipid composition, they may show

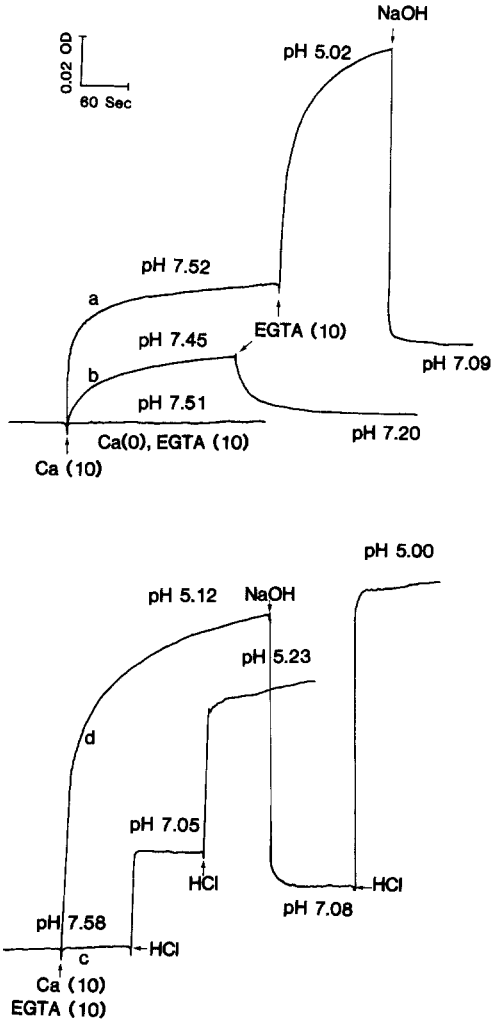

Fig. 11. Addition of 10 mM EGTA to membrane aggregates in the presence of 10 mM Ca^{2+} changed the pH from 7.52 to 5.02 in 10 mM imidazole buffer (a) and from 7.45 to 7.20 in 100 mM imidazole buffer (b). Addition of EGTA in the absence of Ca caused no changes in pH or optical density of the membrane suspension. Tracings c and d were obtained by the addition of mixed solutions of Ca^{2+} and EGTA (numbers in the parentheses indicate the final concentrations of Ca^{2+} and EGTA in the membrane suspension) with and without preadjustment of pH to near 7.5, respectively. Note that the stock solutions of Ca^{2+} and EGTA were preadjusted to near pH 7.5. Adjustments of pH of membrane suspensions was carried out by adding aliquots ($< 20\,\mu l$) of concentrated HCl or NaOH solutions.

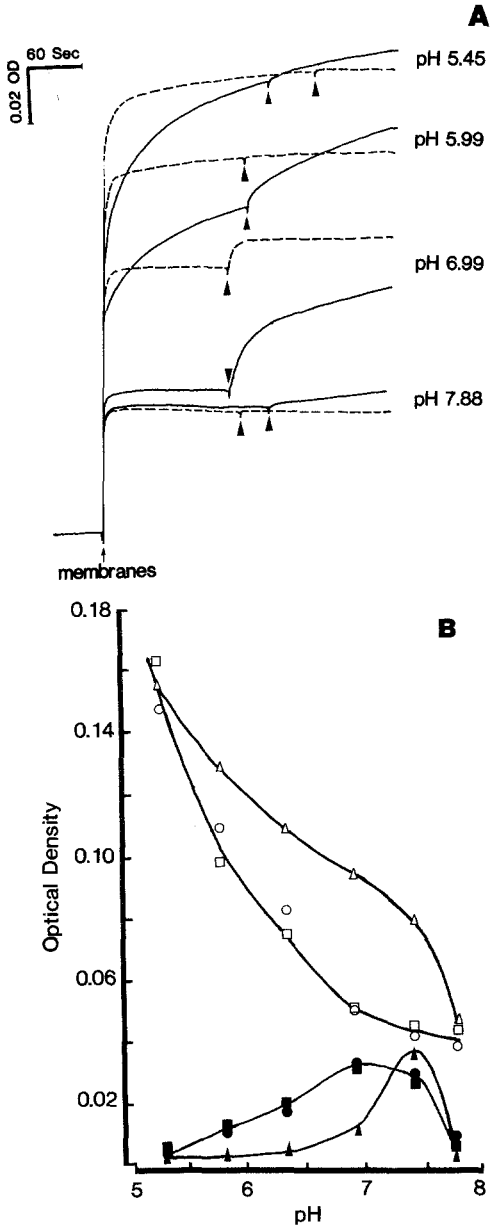

Fig. 12. (A) The effect of pH on the aggregation of microsomal (67.2 μg/ml, solid curves) and mitochondrial (66.9 μg/ml, dashed curves) membranes. Arrow heads indicate the addition of 10 mM Ca^{2+}. (B) pH dependence of membrane aggregation of MIC (circles), F2 (squares) and P1 (triangles). Open symbols: no added Ca^{2+}. Closed symbols: Ca^{2+}-induced aggregation. Optical densities at 450 nm were measured 120 sec after the addition of membranes Ca^{2+}.

a different pattern of pH-dependent membrane aggregation. To test this, the mitochondria-enriched fraction P1, microsomal fraction (MIC), and plasma membrane-enriched fraction (F2) were studied. Figure 12A shows that the pH dependence of the time course of membrane aggregation and the ability of Ca^{2+} to stimulate the membrane aggregation was quite different between P1 and MIC fractions. The patterns of membrane aggregation of F2, being very similar to those of MIC, are not shown. The proton-induced membrane aggregation in the absence of Ca^{2+} and the pH dependence of the Ca^{2+}-induced membrane aggregation of P1, MIC, and F2 are compared in Fig. 12B. In spite of the quantitative differences between P1 and MIC (or F2) fractions, all three membrane fractions qualitatively showed two common features: (a) proton-induced membrane aggregation is more prominent than the Ca^{2+}-induced membrane aggregation; (b) optimal Ca^{2+}-induced aggregation occurs in physiologically relevant pH range (7.0–7.5).

Ca^{2+} Concentration Dependence of Aggregation of Subcellular Membranes

Figure 13 shows the Ca^{2+} concentration of membrane aggregation in P1, MIC, and F2 fractions. It is obvious that F2 and MIC fractions have nearly the same profiles of Ca^{2+} dependence of membrane aggregation with a $K_{0.5}$ for Ca^{2+} of approximately 2 mM, which is similar to the $K_{0.5}$ for Mg^{2+} shown previously (Fig. 4). However, the Ca dependence profile for the P1 fraction appears to be more hyperbolic with a $K_{0.5}$ for Ca^{2+} of only 0.5 mM. The similarity of Ca^{2+} concentration dependence and pH dependence of membrane aggregation of MIC and F2 fractions is in good agreement with our previous finding that the MIC fraction is primarily a plasma membrane-enriched fraction (Kwan *et al.*, 1984b).

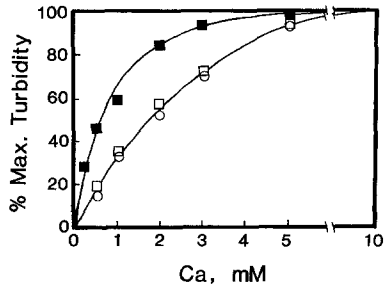

Fig. 13. Ca^{2+} concentration dependence of Ca^{2+}-induced aggregation of MIC (○), F2, (□), and P1 (■). Optical densities were measured 120 sec after the addition of Ca^{2+}. The optical densities at 10 mM Ca^{2+} were taken as 100%.

Cation-Induced Membrane Aggregation as a Preparative Procedure for Plasma Membrane Enrichment

The differential cation-induced aggregation of isolated surface membranes and internal membranes may be useful in selective enrichment of plasma membranes from aortic smooth muscle homogenate. To test this possibility, the aortic postnuclear supernatant (PNS) was equally divided into three portions; one portion served as the control and the other two portions were incubated with 10 mM final concentration of Mg^{2+} and Ca^{2+} separately for 10 min with constant stirring to bring about membrane aggregation. These PNS fractions were then centrifuged as previously described (Kwan *et al.*, 1984b) to obtain MIC fractions. For brevity, only the parameters of MIC fractions from a representative experiment are shown in Table I. It is evident that membrane aggregation was greater in the presence of Mg^{2+} or Ca^{2+}, and the membranes as measured by membrane proteins were shifted from MIC to other fractions, in particular the P1 fraction (not shown), whereas protein contents increased by 3- to 4-fold compared to the control P1. Upon the removal of proteins with cation-induced membrane aggregates, 5′-nucleotidase and Mg^{2+}-ATPase activities were further enriched in MIC, with a concomitant decrease in NADPH-cytochrome *c* reductase and cytochrome *c* oxidase activities. This confirms that the increased turbidity brought about by Mg^{2+} and Ca^{2+} was indeed the membrane aggregation phenomenon and further suggests that the cation-induced membrane aggregation can be utilized as a preparative procedure to enrich plasma membranes from smooth muscle homogenates.

Table I. Protein Content and Membrane Marker Enzyme Activities in MIC Fractions Isolated from the Aortic Muscle Homogenates in the Presence and Absence of 10 mM $MgCl_2$ and $CaCl_2$[a]

Parameters	Control membranes	Mg^{2+} aggregation	Ca^{2+} aggregation
Protein content (% PNS)	7.0	3.2	2.3
5′-Nucleotidase (μmol mg^{-1} h^{-1})	2.9	4.7	5.8
Mg^{2+}-ATPase (μmol mg^{-1} h^{-1})	8.4	15.2	17.5
NADPH-cyt *c* reductase (A_{550} mg^{-1} min^{-1})	0.24	0.10	0.19
Cytochrome *c* oxidase (A_{550} mg^{-1} min^{-1})	1.56	0.12	0.40

[a] Assays for biochemical parameters have previously been described (Kwan *et al.*, 1984b). Total recoveries of protein and enzyme activities were similar and better than 80% for all three groups. See text for details.

Discussion

The present study has demonstrated for the first time that isolated smooth muscle membrane vesicles are capable of eliciting cation-induced aggregation under various experimental conditions. The level of membrane aggregation is governed by many factors including (a) effective charge and concentration of the cations, (b) size of the cations in the case of divalent metal ion-induced membrane aggregation, (c) ionic strength of the medium, (d) polarity of the medium, (e) temperature, (f) pH, and (g) lateral diffusion of the proteins in the plane of the membrane.

Cation-Induced Membrane Aggregation

Based upon studies using model membranes, cations induce membrane aggregation primarily by interacting with the polar heads of negatively charged phospholipids. It is conceivable that trivalent cations with greater effective charge would cause a higher level of membrane aggregation than divalent metal ions. This is supported by our findings that the potency of cations of different valences in stimulating membrane aggregation is in the order $La^{3+} > Mg^{2+} > K^+$ (Fig. 1) and is reciprocally related to the $K_{0.5}$ values for these cations (Fig. 4). For the divalent metal ions, the cation-induced membrane aggregation is a function of the ionic radius, with Cd^{2+} (0.98 Å) being the optimal size. Such a dependence on the effective charge and the ionic radius of the metal ion has also been reported by Ohyashiki *et al.* (1984) using brush border membrane vesicles. The fact that raising the ionic strength of the medium by increasing the concentrations of KCl (Figs. 5 and 6) or imidazole (Fig. 11a) and that decreasing the polarity of the medium by addition of ethanol (Fig. 7) substantially reverse the cation-induced membrane aggregation, are in good agreement with the contention that electrostatic interactions between the positively charged metal ions and negatively charged membrane lipids are the primary forces causing the stimulation of membrane aggregation. This is further supported by the findings that EGTA, a chelator selective for Ca^{2+}, is effective in reversing the Ca^{2+}-induced membrane aggregation (Fig. 11).

The membrane aggregation appears to be dependent upon the degree of freedom of the lateral diffusion of membrane proteins because in the presence of low concentrations of a cross-linking reagent, glutaraldehyde, the cation-induced membrane aggregation is either prevented or rendered irreversible (Fig. 10). Since the lateral diffusion of proteins in the plane of the membrane depends upon the membrane fluidity as well, the stimulating effect of ethanol and increasing temperature (Fig. 8) on the cation-induced membrane aggregation can be partially accounted for by their effects on membrane fluidity.

It should be noted that higher temperature may have an additional effect on the frequency of collisions among membrane vesicles. These combined effects may override the unfavorably lower $K_{0.5}$ for Mg^{2+} at higher temperature (Fig. 9). Nevertheless, the role of membrane fluidity in cation-induced smooth muscle membrane aggregation requires further studies using other biophysical methods, such as spectrofluorometric techniques (Ohyashiki and Mohri, 1983).

Proton-Induced Membrane Aggregation

As the pH of the membrane suspension decreases, the membrane aggregation becomes progressively increased and the Ca^{2+}-inducible aggregation diminishes (Fig. 12), presumably as a result of neutralization, by protons, of the negatively charged groups of the membrane lipids as well as proteins. This result suggests that the "isoelectric point" of the smooth muscle membranes is in the acidic region ($<$ pH 5.5). This is in sharp contrast to the finding using intestinal brush border membrane vesicles that Ca^{2+}-induced membrane aggregation is independent of pH (Ohyashiki *et al.*, 1984). Such different patterns of pH dependence of aggregation of biological membranes may underscore possible differences in their cell membrane compositions (see below). Since the mitochondrial membranes and plasma membranes of aortic smooth muscle also differ in their protein (Kwan *et al.*, 1984b) and perhaps lipid composition, their different time course (Fig. 12A) and pH profiles (Fig. 12B) of membrane aggregation in the presence and absence of Ca^{2+} and different $K_{0.5}$ for Ca^{2+} (Fig. 13) are not unexpected.

Proton-induced aggregation or fusion of phospholipid vesicles has also been reported (McDonald *et al.*, 1976; Bondeson *et al.*, 1984). McDonald *et al.* (1976) found that proton-induced fusion of phosphatidylserine vesicles occurs as the pH is lowered to less than 4.5. They suggested that protonation of serine carboxyl group is involved in this process. Bondeson *et al.* (1984) showed that fusion occurs in glycolipid–phospholipid vesicles containing phosphatidate and phosphatidylethanolamine as pH is lowered from 7.4 to less than 6.5. Our finding is very similar to their observation. The general consensus from the model membrane and biological membrane studies is that proton-induced membrane aggregation is highly dependent upon the nature of membrane phospholipids.

Using a stop-flow turbidimetric technique, Lansman and Haynes (1975) have shown that aggregation of lipid vesicles is the primary determinant of the fusion reaction, and the Ca^{2+}-induced lipid membrane aggregation is effected by Ca^{2+}-mediated salt bridges. This charge-shielding effect of Ca^{2+} via salt bridges may be operationally similar to the effect of acidification which "shields" the negative charges of the membrane via protonation.

Aggregation of Plasma Membranes and Internal Membranes

Studies of membrane aggregation using biological membranes are very few and we are not aware of any work comparing the properties of aggregation of membrane vesicles derived from different subcellular structures. The membrane fraction enriched in internal membrane structures (although it was termed mitochondrial membrane fraction P1, it also contained a substantial amount of endoplasmic reticulum vesicles and lyzosomes; Kwan *et al.*, 1984b) showed a distinct pattern of membrane aggregation different from that of plasma membrane-enriched fraction F2 in three aspects: (a) the rate of membrane aggregate formation, (b) the pH profile of membrane aggregation, and (c) the $K_{0.5}$ for Ca^{2+}. Such differences may reflect the differences in their membrane composition as discussed previously. Such a differential aggregation is also applicable as a fractionation technique to effectively separate internal membranes from the plasma membranes in smooth muscle homogenate (Table I). Such an application has recently been reported as well in a preliminary study of Na^+/H^+ exchange across the membrane vesicles using dog mesenteric arteries (Kahn *et al.*, 1986). The fact that aggregation of isolated mitochondrial and plasma membranes was similar in the presence of 10 mM Mg^{2+} or Ca^{2+} (Fig. 13) whereas 10 mM Mg^{2+} or Ca^{2+} added to the tissue homogenate was able to achieve effective separation of these membranes, deserves some comments. Firstly, the tissue homogenate contained a much higher concentration of proteins and more heterogenous membranes than the isolated fractions; thus, the "effective concentration" of Ca^{2+} or Mg^{2+} to cause membrane aggregation may be considerably lower than 10 mM. Secondly, since membrane fractions were separated by differential centrifugation based upon mass difference of the membrane particles, under the same centrifugal force or even with the same degree of aggregation, the sedimentation velocity is expected to be greater for aggregated mitochondia than aggregated plasma membrane vesicles.

The physiological significance of the membrane aggregation reported in the present work is not known, although it is likely to be associated with membrane fusion, which is stimulated by Ca^{2+} in some cases and by acidification in others (White and Helenius, 1980; White *et al.*, 1981; Tycko and Maxfield, 1984). Our present knowledge of the membrane processes involved in the endocytosis and exocytosis of smooth muscle cell membrane is too meager to allow us to put our present observations into physiological prospective. In any event, this work provides a basis for the fundamental interactions between biological membranes under various conditions which are of physiological relevance and suggests a novel as well as rapid method for the preparation of vascular smooth muscle plasma membranes. Application toward the use of such membrane preparation in the study of ion

binding and transport, ligand–receptor interactions, and surface membrane enzymes is currently in progress in this laboratory.

Acknowledgment

This work was supported by a grant from the Canadian Diabetes Association. C. Y. Kwan is a senior research fellow of the Heart and Stroke Foundation of Ontario. Critical comments and helpful suggestions from Dr. E. E. Daniel and technical assistance from Mrs. V. Gaspar are highly appreciated.

References

Bondeson, J., Wijkander, J., and Sundler, R. (1984). *Biochim. Biophys. Acta* **777**, 21–27.
Daniel, E. E., Grover, A. K., and Kwan, C. Y. (1982). *Fed. Proc.* **41**, 2898–2904.
Gabella, G. (1981). In: *Smooth Muscle*: An Assessment of Current Knowledge (Bulbring, E., Brading, A. F., Jones, A. W., and Tomita T., eds.), Edward, London.
Grover, A. K., Kwan, C. Y., Kostka, P., Sheppard, S. M., and Daniel, E. E. (1984). *Can. J. Physiol. Pharmacol.* **62**, 1203–1208.
Haynes, D. H., Lansman, J., Cahill, A. L., and Morris, S. J. (1979). *Biochim. Biophys. Acta* **557**, 340–353.
Kahn, A. M., Shelat, H., and Allen, J. C. (1986). *Am. J. Physiol.* **250**, H313–H319.
Kitabgi, P., Kwan, C. Y., Fox, J. E. T., and Vincent, J. P. (1984). *Peptides* **5**, 917–923.
Kwan, C. Y., and Kostka, P. (1983). *Mol. Physiol.* **3**, 265–275.
Kwan, C. Y., and Kostka, P. (1984). *Biochim. Biophys. Acta* **776**, 209–216.
Kwan, C. Y., Kostka, P., and Ramlal, T. (1984a). *Mol. Physiol.* **6**, 99–114.
Kwan, C. Y., Triggle, C. R., Grover, A. K., Lee, R. M. K. W., and Daniel, E. E. (1984b). *J. Mol. Cell. Cardiol.* **16**, 747–764.
Lansman, J., and Haynes, D. H. (1975). *Biochim. Biophys. Acta* **394**, 335–347.
MacDonald, R. C., Simon, S. A., and Baer, E. (1976). *Biochemistry* **15**, 885–891.
Morris, S. J., Chiu, V. C. K., and Haynes, D. H. (1979). *Membr. Biochem.* **2**, 163–202.
Ohyashiki, T., and Mohri, T. (1983). *Biochim. Biophys. Acta* **731**, 312–317.
Ohyashiki, T., Takeuchi, M., and Mohri, T. (1984). *J. Biochem.* **95**, 881–886.
Papahadjapoulos, D., Poste, G., and Vail, W. J. (1979). In: *Methods in Membrane Biology* (Korn, E. D., ed.), Vol. 10, Plenum Press, New York and London, pp. 1–121.
Tycko, B., and Maxfield, F. R. (1984). *Cell* **28**, 643–651.
White, J., and Helenius, A. (1980). *Proc. Natl. Acad. Sci. USA* **77**, 3273–3277.
White, J., Matlin, K., and Helenius, A. (1981). *J. Cell Biol.* **89**, 674–679.
Wilshut, J., Duzgunes, N., and Paphadigopoulos, D. (1981). *Biochemistry* **20**, 3126–3133.